

# An Endfire Beam-Switchable Antenna Array Used in Vehicular Environment

Fei Liu, Zhijun Zhang, *Senior Member, IEEE*, Wenhua Chen, *Member, IEEE*, Zhenghe Feng, *Senior Member, IEEE*, and Magdy F. Iskander, *Fellow, IEEE*

**Abstract**—An endfire beam-switchable antenna array, which is designed for vehicular mobile application regulated by the IEEE 802.11p standard, is proposed in this letter. The antenna is a linear array with four L-shaped elements separated by a quarter of a wavelength. The horizontal beams of L-elements point to four different directions, and this reduces the antenna height, decreases the mutual coupling between elements, and also eliminates the blind zone in the broadside direction. The antenna array has two isolated ports. By switching between two ports, the endfire radiation pattern can be switched toward opposite directions. A prototype antenna is built to verify the concept. The gain of the prototype is better than 6 dBi, and the impedance matching is better than  $-14$  dB in the working band (5.850–5.925 GHz).

**Index Terms**—Endfire antenna array, switchable beam, vehicular antenna.

## I. INTRODUCTION

VEHICULAR land transportation has become an indispensable and necessary element of contemporary society activities. However, the vehicle transportation environment has been facing severe situations with increasing number of accidents and congestions in many metropolitan areas and highways worldwide. This necessitates the adaptation of intelligent transportation system (ITS) that could improve vehicle driving environment with respect to safety, efficiency, and information availability. This demand leads to wireless access for vehicular environments (WAVE) [1], which is also regulated by the IEEE 802.11p standard. WAVE systems operate in 5.850–5.925 GHz frequency band assigned by the Federal Communications Commission (FCC). The advanced orthogonal frequency-division multiplexing (OFDM) modulation is adopted to achieve high-speed data rates up to 6–27 Mbs/s.

Manuscript received November 06, 2009; revised December 29, 2009; accepted January 20, 2010. Date of publication March 11, 2010; date of current version April 05, 2010. This work supported in part by the National Basic Research Program of China under Contract 2009CB320205, the National High Technology Research and Development Program of China (863 Program) under Contract 2007AA01Z284, and the National Natural Science Foundation of China under Contract 60771009.

F. Liu, Z. Zhang, W. Chen, and Z. Feng are with the State Key Lab of Microwave and Communications, Department of Electronic Engineering, Tsinghua University, Beijing 100084, China (e-mail: liufei02@gmail.com; zjzh@tsinghua.edu.cn; chenwh@tsinghua.edu.cn; fzh-dee@tsinghua.edu.cn).

M. F. Iskander is with the Hawaii Center for Advanced Communications (HCAC), University of Hawaii at Manoa, Honolulu, HI 96822 USA (e-mail: iskander@spectra.eng.hawaii.edu).

Color versions of one or more of the figures in this letter are available online at <http://ieeexplore.ieee.org>.

Digital Object Identifier 10.1109/LAWP.2010.2044973

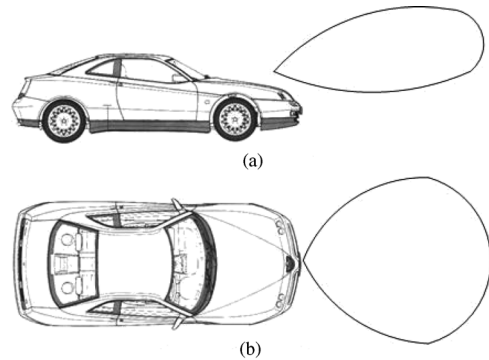


Fig. 1. An ideal radiation pattern in the forward direction. (a) Side view and (b) top view of an ideal pattern.

In an 802.11p system, access points (APs) are installed along the road and, hence, are either in front or behind a moving vehicle. An antenna that is specifically tailored for this kind of application should provide two switchable beams, one toward the front and one toward the back of the vehicle. A car can use its forward beam to connect an AP in front of it and switches to the backward beam after it passes the AP to maintain the good connection.

Fig. 1 shows what an ideal pattern should look like in 802.11p systems. Because the roadside AP is far away most of the time, the radiation pattern needs to have a narrow beamwidth in the elevation plane. In the azimuth plane, the road system is not always perfectly straight, and vehicles also need to change lanes from time to time, so the radiation pattern needs to have certain beamwidth in this plane to guarantee a stable connection to the roadside AP.

In all antenna array configurations, the endfire array is the best candidate to generate the ideal pattern shown in Fig. 1. Unlike broadside array, an endfire array could be designed to have only one peak in the azimuth plane, thus eliminate the requirement of a reflector. By selecting the total number of array elements, the beamwidth in the azimuth plane can be easily adjusted. Endfire arrays have been investigated for many years and may include Yagi and log-periodic antennas [2]. Wideband antenna elements have been used in the designs of endfire arrays. Diamond-shape dipoles have been used to achieve 100% bandwidth with a stable endfire pattern [3]. Fan-shaped bow-tie antennas can also be used to achieve an endfire radiation [4]. In both [3] and [4], grounds are used as the reflector to improve the front-to-back ratio of the antenna. Therefore, they are only suitable for fixed beam application. Drossos *et al.* [5] proposed a bidirectional endfire array, which radiates at both endfire directions. Its gain is around 3 dB lower than a unidirectional

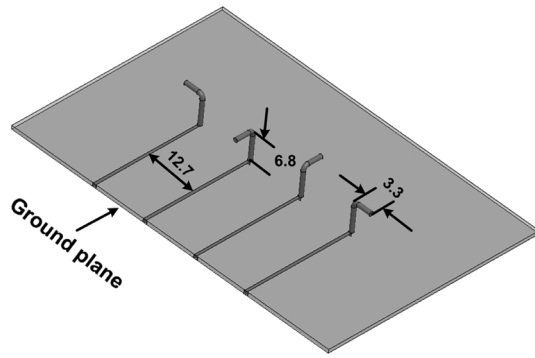


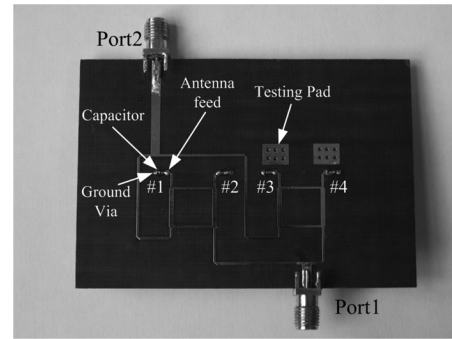
Fig. 2. Simulation model of the antenna array (in mm).

array. Kamarudin *et al.* [6] proposed a switch beam array that can cover all azimuth angles; to achieve that capability, a complex feeding network and multiple switches must be used. The endfire array proposed in this letter is an improved version of endfire beam switchable array proposed in [7], which is a linear array with four L-shaped elements separated by a quarter of a wavelength. The feed network of the array has two isolated inputs and four outputs. Each input can generate equal amplitude signals with  $90^\circ$  incremental or descending phase distribution on four output ports, thus forming two orthogonal endfire radiation patterns as will be described in the following sections.

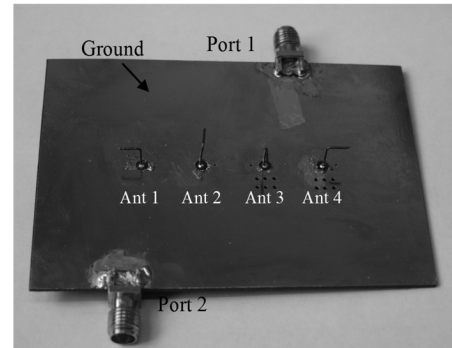
## II. DESIGN APPROACH

As shown in Fig. 2, the proposed array is a quarter-wavelength-separation linear array. It consists of four L-shaped elements instead of monopole antennas to decrease the overall height. The horizontal beam of each L-element points to a different direction, thus reducing the mutual coupling between adjacent elements. In 802.11p systems, the AP might be located just on top of the vehicle. If monopole array elements are used or horizontal beams of all L-elements are parallel to each other, there will be a deep null in the broadside direction. The rotational arrangement of the horizontal beams proposed in this letter can eliminate this deep null and improve the overall quality of connections with APs along the road.

Fig. 3(a) shows the back view of the prototype array. The feeding network can be clearly observed from this side. The circuit is composed of two 3-dB branch-line  $90^\circ$  hybrid couplers, whose port impedance is  $100\ \Omega$ , and a microstrip line power distribution network. The feeding network has two isolated input ports, which are ports 1 and 2, and four output ports, which are numbered from antenna 1 to 4. When fed from Port 1, the  $50\text{-}\Omega$  input microstrip line is split to two  $100\text{-}\Omega$  microstrip lines by a T-junction first, and then connected to directional couplers 1 and 2, respectively. The microstrip line that connects to directional coupler 1 is a half-wavelength shorter than the line that connects to directional coupler 2, and this generates a  $180^\circ$  phase delay at directional coupler 2 at 5.9 GHz. When fed from the top-left port of either directional coupler, the output signal from the bottom-right port has a  $90^\circ$  phase delay compared to the bottom-left port. Combining phase delays from the feeding network and directional couplers, the output signal at antenna 1 to 4 has a descending phase distribution with a  $90^\circ$  difference be-



(a)



(b)

Fig. 3. Photographs of fabricated endfire array: (a) back view and (b) front view.

tween adjacent elements. It is easy to see that the amplitudes of output signal at antenna 1 to 4 are all equal.

As the space separation between the array elements is also  $90^\circ$ , thus the signal distribution on antenna 1 to 4 when Port 1 is fed can generate an endfire radiation pattern with peak points from antenna 1 to antenna 4. When Port 2 is fed, the phase relationship between adjacent elements will be reversed, which generates an endfire pattern pointing to the opposite direction, which means from antenna 4 to antenna 1.

## III. MEASUREMENT RESULTS

The printed circuit board (PCB) is made of low-loss RF laminate material with a permittivity of 2.3. The size of the PCB is  $80 \times 60\ \text{mm}^2$ . The detailed antenna array dimension can be found in Fig. 2. The distance between adjacent elements is 12.7 mm, which is a quarter of a wavelength in free space at 5.9 GHz. The L-shape element is made of copper wire with a diameter of 0.35 mm. The vertical segment is 6.8 mm long, and the horizontal beam is 3.3 mm long. The input impedance of each antenna was tuned to  $100\ \Omega$  by adjusting the total length of the antenna and the value of a shunt capacitor as shown in Fig. 3(a). The capacitance of those components is 1.8 pF in the current design. There are two ground patches in Fig. 3(a), which are used for testing purposes only and do not have any function in the finished prototype.

Shown in Fig. 4 are simulated phases at four antennas when they are fed from Port 2. The phase difference between adjacent ports is  $90^\circ$  at 5.9 GHz, which is required to generate an endfire radiation pattern.

To verify the design of the feeding circuit by itself, four antennas are removed and replaced by four  $100\text{-}\Omega$  resistors.

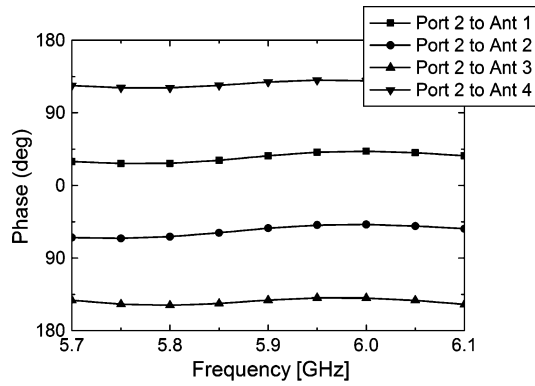


Fig. 4. Simulated phases at antennas when fed from the Port 2.

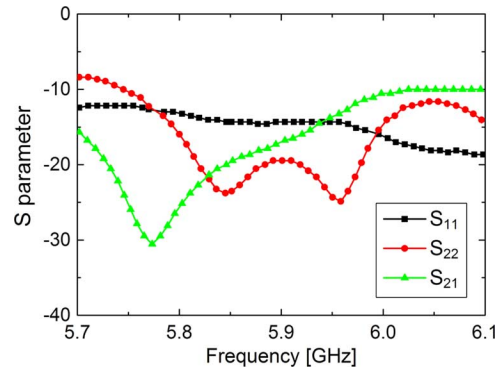


Fig. 6. Measured S-parameters of the whole array.

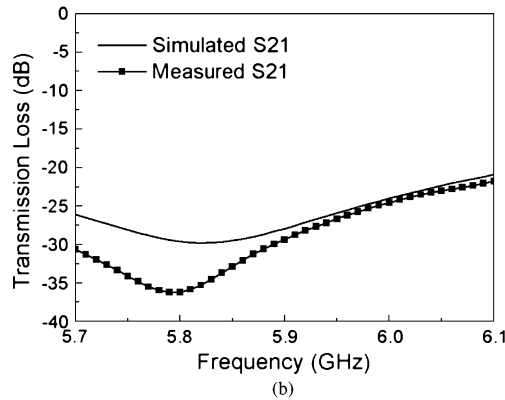
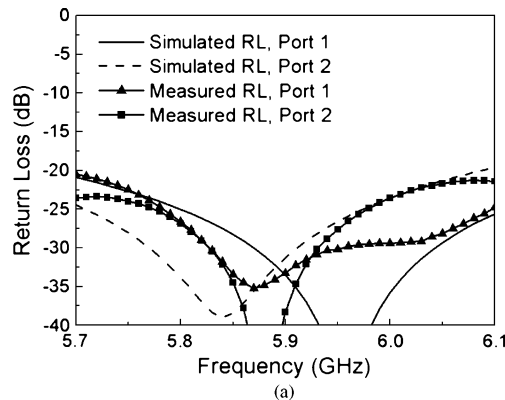
Fig. 5. Simulated and measured S-parameters at both ports 1 and 2 when all four antennas are replaced by 100- $\Omega$  resistors. (a) Return loss. (b) Transmission loss (S21).

Fig. 5(a) shows the simulated and measured return loss at both ports 1 and 2. Although all return losses are below  $-20$  dB, the difference between simulation and measurement at Port 1 is larger than at Port 2. Shown in Fig. 5(b) are the simulated and measured results of S21.

Fig. 6 shows the measured S parameters between ports 1 and 2 after the entire array is assembled. In the working band, the return loss of ports 1 and 2 is better than  $-21$  and  $-14.5$  dB, respectively. The isolation between ports 1 and 2 is better than  $-15.5$  dB. Comparing the result of the full array to the results of the feeding network terminated by 100  $\Omega$ , it is clear that four handmade antenna elements are not ideally 100  $\Omega$ .

Fig. 7 shows the simulated and measured array gain. The solid line represents the simulated results using HFSS software. In the

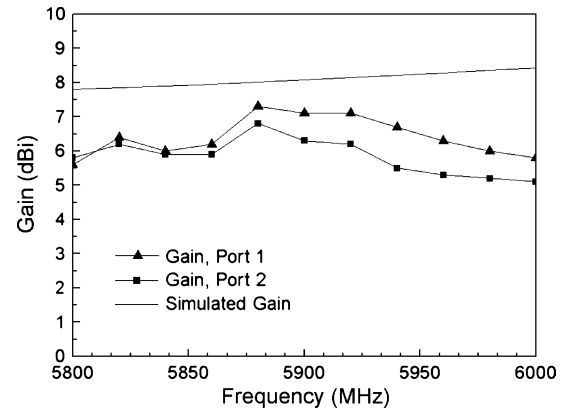


Fig. 7. Simulated and measured array gain.

simulation, the impact of the feeding networking is not included. The simulation model has only the four-port antenna array as shown in Fig. 2 with a lumped matching capacitor attached to each port. The ground has limited size, which is  $60 \times 80$  mm<sup>2</sup>. All ports use 100  $\Omega$  as input impedance, and each port is excited by the same amplitude but 90° phase shift with respect to the adjacent port. The simulated results show the best achievable antenna gain when all antennas are identical and when there is no mismatch at the antenna port. Due to the symmetric property of the array configuration, the simulated gain when either Port 1 or 2 is excited is the same. The lines with triangle markers and square markers in Fig. 7 are for measured antenna gain when Port 1 and Port 2 are excited, respectively. Over the entire working band, the array gain is better than 6 dBi. When the array is excited from Port 1, the measured antenna gain is about 1 dB lower than the simulated result. This means that the array efficiency is 80%. When excited from Port 2, the efficiency is around 65%. The extra 15% efficiency loss may be contributed to mismatch in the feeding network. At 5.9 GHz, the feeding network does have noticeable loss.

Fig. 8 shows the measured 3D radiation pattern at 5.9 GHz when the array is excited from Port 1 and 2, respectively. The two radiation patterns are similar in shape and point toward opposite directions. These patterns have narrow beamwidth in the elevation plane (57°) and wide beamwidth in the azimuth plane (130°), which is suitable for the 802.11p applications. Clearly, these beamwidths could be further reduced and the array gain further increased by including additional elements in the array.

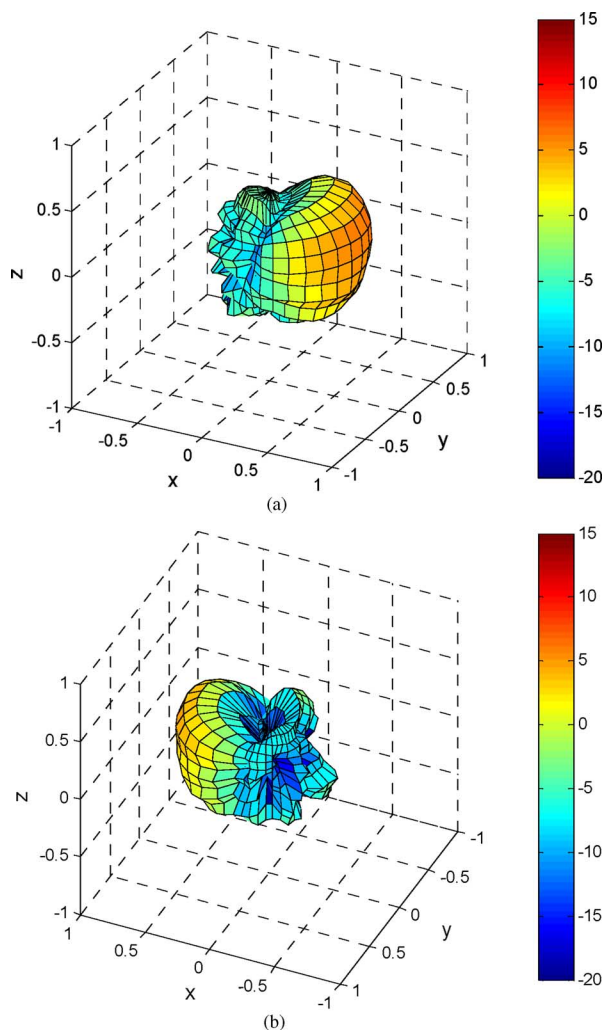


Fig. 8. Measured 3D radiation pattern at 5.9 GHz for (a) Port 1 and (b) Port 2.

#### IV. CONCLUSION

An endfire phased array, which can be used in IEEE 802.11p systems, is proposed in this letter. The array is capable of switching between two radiation beams in opposite endfire directions and can hence provide suitable performance for vehicular mobile applications. A prototype antenna was manufactured and measured. The prototype has a gain better than 6 dBi and a matching better than  $-14$  dB in the working IEEE 802.11p band (5.850–5.925 GHz).

#### REFERENCES

- [1] W. Xiang, P. Richardson, and J. Guo, "Introduction and preliminary experimental results of Wireless Access for Vehicular Environments (WAVE) systems," in *Proc. 3rd Annu. Int. Conf. Mobile Ubiquitous Syst., Netw. Services*, Jul. 2006, pp. 1–8.
- [2] C. A. Balanis, *Antenna Theory. Analysis and Design*. New York: Wiley, 1982.
- [3] A. Eldek, "A 100% bandwidth microstrip antenna with stable endfire radiation patterns for phased array applications," in *Proc. IEEE Int. Symp. Antennas Propag. & URSI Nat. Radio Sci. Meeting*, Albuquerque, NM, Jul. 2006, pp. 3751–3754.
- [4] S. Qu, J. Li, Q. Xue, and C. Chan, "Wideband periodic endfire antenna with bowtie dipoles," *IEEE Antennas Wireless Propag. Lett.*, vol. 7, pp. 314–317, 2008.
- [5] G. Drossos, Z. Wu, and L. E. Davis, "Two-element endfire dielectric resonator antenna array," *Electron. Lett.*, vol. 32, no. 7, pp. 618–619, Mar. 1996.
- [6] M. Kamarudin and P. Hall, "Disk-loaded monopole antenna array for switched beam control," *Electron. Lett.*, vol. 42, no. 2, pp. 66–68, Jan. 2006.
- [7] Z. Zhang, F. Liu, W. Chen, Z. Feng, and W. Xiang, "An endfire phased array used in wireless access for vehicular environments (WAVE)," in *Proc. Int. Conf. Microw. Millim. Wave Technol.*, Nanjing, China, 2008, vol. 1, pp. 428–431.